

Dimerisation, electronic structure, and magnetic properties in $\text{Ba}_6\text{Cr}_2\text{S}_{10}$ compounds: First principles studies

Jianfeng Zhang^{1,*}, Huancheng Yang^{2,†} and Wei Wu^{3,4‡}

¹*Beijing National Laboratory for Condensed Matter Physics,*

Institute of Physics, Chinese Academy of Sciences, Beijing 100190, China

²*Key Laboratory of Quantum State Construction and Manipulation (Ministry of Education), Renmin University of China, Beijing, 100872, China*

³*UCL Department of Physics and Astronomy and London Centre for Nanotechnology, University College London, Gower Street, London WC1E 6BT and*

⁴*UCL Institute for Materials Discovery, University College London, Malet Place, London, WC1E 7JE*
(Dated: April 14, 2023)

Quasi-one-dimensional systems are fascinating as they can exhibit very rich and interesting physics. The spin chain compound $\text{Ba}_6\text{Cr}_2\text{S}_{10}$ has been synthesised experimentally under extreme conditions recently, which has shown interesting magnetic and toroidal properties due to dimerisation. Here we have performed first principles calculations to compute the electronic structure and magnetic properties of $\text{Ba}_6\text{Cr}_2\text{S}_{10}$, which are consistent with the experimental results for the magnetic structure and properties shown in [Zhang, et al, Adv. Mat. 34 (12), 2106728 (2022)]. Moreover, based on our calculations, we can find more interesting physics, including (i) the small size of the Hubbard U parameter that implies the screening effect of surrounding Ba atoms, (ii) the dimerisation of Cr atoms mainly induced by the sulfur ligands, and (iii) the next-nearest-neighbouring anti-ferromagnetic interaction along the spin chain, which could bring forward spin frustration, thus spin liquid.

I. INTRODUCTION

Quasi-one-dimensional (quasi-1D) magnetic systems can give rise to many interesting phenomena in condensed matter physics such as quantum spin liquid [1]. In one dimension, quantum fluctuations become important as compared with thermal fluctuations at sufficiently low temperature environment and can be manifested in quantum spin liquid[1], quantum tunnelling [2], fractional edge states [3], and topological order [4, 5]. 1D spin chains can provide a fascinating physical platform not only to the study of low-dimensional physics but also long-range quantum entanglement [6, 7]. In addition, one-dimensional Majorana zero-mode bound states share the same central charge of $\frac{1}{2}$ with that in one-dimensional Ising model with transverse magnetic field [8, 9]. One of the most interesting temperature regions is probably where the three dimensional ordering is not yet established but the temperature is lower than the Curie intercept θ_p originating from the exchange interaction in quasi-1D spin chains, which could lead to quantum spin liquid [1]. In addition, quasi-1D spin chains can also be used to realize polar toroidal moments in solid state - an interesting dipole moment that violates both the spatial and time inversion symmetries [10–12]. Magnetic toroidal moments can be found in ordered spin systems, for example in 1D [10, 12], orbital loop current [13, 14], and wheel-shaped molecules such as Dy_6 [15, 16].

In quantum information processing, quantum communications through 1D anti-ferromagnetic spin chains have been proposed to realise quantum state transfer between the chain ends [17].

Recently the compounds consisting of spin chains, either organic or inorganic, have attracted much attention for magnetism and spintronics. Organic spin-chain compounds, in which spin chains can weakly interact with each other, can form in phthalocyanine-based molecular chains such as cobalt phthalocyanines [18–26]. More broadly speaking, organic single chain magnets, which can explore chemical synthesis and different building blocks for magnetic spin units, have similar functionalities to single molecule magnets, thus pointing to many potential applications in spintronics and quantum computing [27]. There are many molecular material candidates for single chain magnets, such as $[\text{Mn}(\text{TPP})\text{O}_2\text{PPhH}]\cdot\text{H}_2\text{O}$ (TPP = meso-tetraphenylporphyrin). For inorganic compounds, the AMX_3 and $\text{B}_3\text{MM}'\text{O}_6$ ($\text{A} = \text{Cs/Rb}$, $\text{B} = \text{alkaline-earth metal}$, $\text{M/M}' = \text{transition metals}$, $\text{X} = \text{halides}$) compounds form large families of spin chain compounds, which have exhibited interesting low-dimensional magnetic behaviour, as observed in neutron scattering experiments [28–30]. CsCoBr_3 and $\text{Ca}_3\text{Co}_2\text{O}_6$ consist of strongly coupled Ising chains, which are vertical to the triangular lattice plane[31]. The spins in the chain in CsCoBr_3 are anti-ferromagnetically coupled, while those in $\text{Ca}_3\text{Co}_2\text{O}_6$ are ferromagnetically arranged [31]. Especially the $\text{B}_3\text{MM}'\text{O}_6$ compound family has complex magnetic structures, multiple exchange interactions between spins on the transition-metal ions. In some compounds, $4d/5d$ orbitals will be involved, which implies that the spin-orbit interaction will play an im-

*Electronic address: zjf@iphys.ac.cn

†Electronic address: hcyang@ruc.edu.cn

‡Electronic address: wei.wu@ucl.ac.uk

portant role, such as the spin anisotropy [30]. For $B_3MM'O_6$ compounds, Sr_3ZnRhO_6 [32], Sr_3CuIrO_6 [33], Sr_3CuRhO_6 [34], Ca_3CoRhO_6 [35], and Sr_3NiIrO_6 [30] have been extensively studied, showing interesting magnetic properties such as magnetisation jumps.

Hf_5Sn_3Cu -anti type ternary compounds A_3BX_5 (A = alkali earth metal, B = transition metal and X = chalcogen) are a typical spin chain compound family that also are candidates for one-dimensional ferrotoidic chains [11, 12]. Here we report the theoretical studies from first principles for a newly synthesized spin-chain compound $Ba_6Cr_2S_{10}$ (BCS) under high-pressure and high-temperature conditions. In terms of chain structures, BCS has the face-sharing octahedral formed by sulfur atoms (Fig.1), which is similar to the AMX_3 and $B_3MM'O_6$. The dimerisation induced mainly by the octahedron formed by the S atoms will lead to spin anisotropy and ferro-toroidic ground state. In addition, our calculations show an orbital ordering on Cr atoms along the chain due to the peculiar face-sharing octahedral structure. The remaining discussion falls into three sections. In §II, we introduce the computational methods. In §III, we present our results and discuss them. In §IV, we draw some general conclusions.

II. METHODS

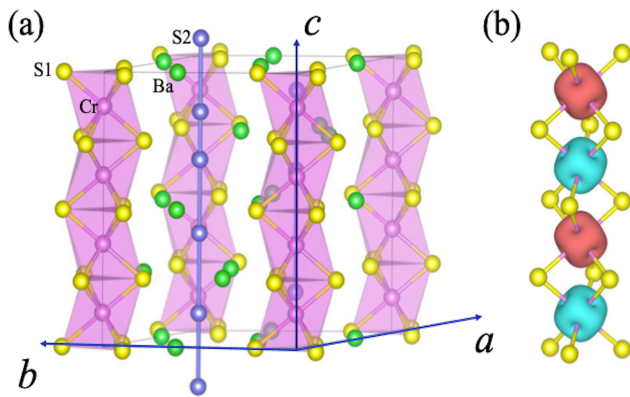


FIG. 1: (Colour online.) (a) The crystal structure of BCS is shown. Ba is in green. Cr is in pink. S is in yellow. Cr atoms, bonded by S atoms, form chains along the c -axis. (b) The orbital ordering on Cr along the chain. Due to the zig-zag ligand, the Cr orbitals will alternate along the c -axis. Here in (a), S1, S2, and Cr label the atoms for the projected band structures. In (a) we have also shown the dimerisation of Cr atoms, induced by the S ligands.

First-principles density-functional-theory calculations have been performed to study the electronic structure and spin anisotropy of the system using the projector augmented wave (PAW) method [36] as implemented in the VASP package [37, 38]. The standard

generalised-gradient approximation for the exchange-correlation functional - Perdew-Burke-Ernzerhof (PBE) - has been chosen for all the calculations [39]. The kinetic energy cutoff of the plane-wave basis was set to be 350 eV. A $16 \times 16 \times 12$ k-point mesh was used for the Brillouin zone (BZ) sampling. The Fermi level was broadened by the Gaussian smearing method with a width of 0.05 eV. The SCF converging process is accelerated by a linear mix of 10%. The Vanderbilt ultra-soft pseudo-potentials developed for the PBE exchange-correlation functional have been used for Ba, Cr, and S, throughout all the DFT + U calculations. The band structure was plotted as the high-symmetry points in the first Brillouin zone of a hexagonal lattice, i.e., $\Gamma(0,0,0) \rightarrow M(\frac{1}{2},0,0) \rightarrow K(\frac{2}{3},\frac{1}{3},0) \rightarrow \Gamma(0,0,0) \rightarrow A(0,0,\frac{1}{2}) \rightarrow L(\frac{1}{2},0,\frac{1}{2}) \rightarrow H(\frac{2}{3},\frac{1}{3},\frac{1}{2}) \rightarrow \Gamma(0,0,0)$.

BCS has hexagonal lattice structure in which the spin chain consisting of Cr atoms is along the c -axis, as shown in Fig.1(a). The symmetry group for BCS is $P62c$. The lattice parameters are $a = b = 9.1371\text{\AA}$, $c = 12.3175\text{\AA}$, $\alpha = \beta = 90^\circ$, and $\gamma = 120^\circ$. In our VASP calculations, the lattice constants and internal atomic positions were allowed to relax until all the forces on atoms were smaller than 0.01 eV/\AA . Our optimal lattice constants is: $a_o = b_o = 9.27\text{\AA}$ and $c_o = 12.44\text{\AA}$, which well agrees with the experimental measurements [12]. In our study, the GGA functional was employed because the present results ($\sim 1.2 \text{ eV}$) can well describe the experiment observed energy gap [12]. The spin-orbit interaction (SOI) was included for the spin-polarized calculation to understand the non-collinear magnetic configuration in the ground state. The U-parameter has also been added (DFT+U) to work out the exchange interactions. We have computed the intra-chain nearest-neighbouring (NN) and next-nearest-neighbouring (NNN) and inter-chain NN exchange interactions. A set of values of $U = 0$ to 2 eV with an increments of 0.5 eV were used for the DFT+U calculations. By comparing with the experimental band gap, we can determine the optimal value for the Hubbard U -parameter.

III. RESULTS AND DISCUSSION

We have presented the band structure for BCS with (a) and without (b) dimerisation in Fig.2. In (a), we show the band structure for dimerised BCS, in which the Cr atoms and their surrounding S ligands form dimer along the c -axis (the chain direction). The dimerisation lattice parameters were taken from the experimental value from Ref.[12] In Fig.2(b), by contrast, for the BCS structure without dimerisation, we can see a large dispersion originating from S atoms across the band gap. The band dispersion across the Fermi surface is along $\Gamma(0,0,0) \rightarrow A(0,0,\frac{1}{2})$, which is in the chain direction, which is consistent with the dimerization along the c -axis. This is a typical characteristics for the Peierls transition, i.e., the dimerisation of S ligands will

open up a band gap as compared with the case without dimerisation. The dimerisation would also bring forward charge density waves (CDW), which can be seen clearly in Fig.1(b). Therein, not only charge ordering but also orbital ordering can be formed due to the zig-zag lattice formation along the chain.

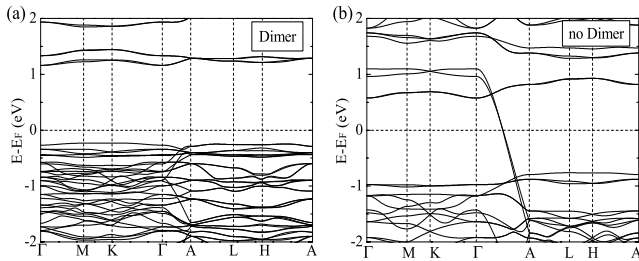


FIG. 2: (Colour online.) A comparison between the band structures of the crystal structures with dimerised Cr atoms and without. We can clearly see the pronounced Peierls transition, which is due to the S ligands rather than Cr atoms.

We have also computed the spin-polarised projected band structure for BCS, as shown in Fig.3. The spin-up band structures are plotted in (a) and (c), while the spin-down band structures are plotted in (b) and (d). The band structure projected onto the Cr atoms for spin up is shown in (a), in which the dominant projections are at $E - E_F \sim -0.2$ eV, i.e., 0.2 eV below the Fermi surface. The projection to the atom S1 and S2 atoms labelled in Fig.1(a) suggests that S atoms contribute to the same energy range as Cr atoms, thus leading to strong hybridisation between Cr and S. In Fig.1(b), we can see the orbital ordering on Cr atoms, which is mainly caused by the sulfur ligands, further confirming the importance of S atoms in the dimerisation.

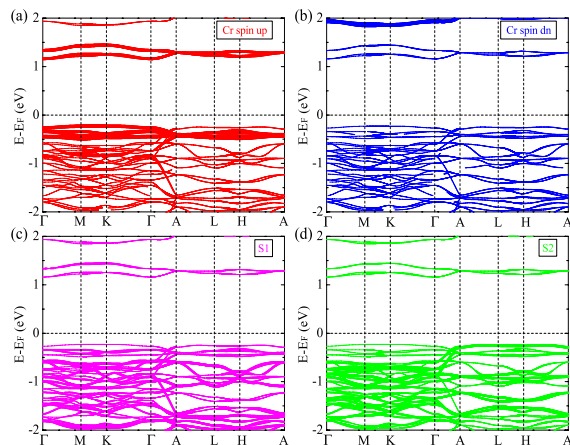


FIG. 3: (Colour online.) The spin-polarised band structures projected to Cr and S, which clearly dominates the bands near the Fermi energy.

TABLE I: Our calculated MAE of the magnetic moment on the Cr atoms. Three typical directions, [001], [110], and [100] were carried out. The exhibited energies are relative to the [001] direction with unit of meV/Cr.

Direction	[001]	[110]	[100]
ΔE	0.0	-0.023	-0.098

TABLE II: Exchange interaction.

U (eV)	0	0.5	1.0	1.5	2.0
J_{NN} (meV)	15.0	11.6	8.9	6.7	4.9
J_{NNN} (meV)	2.2	1.4	0.9	0.5	0.3
$J_{\text{Inter-chain}}$ (meV)	-0.03	-0.02	-0.01	-0.01	-0.01

In the studies of the magnetic anisotropic energy (MAE) on the Cr atoms, the spin-orbital interaction (SOI) interaction was also included with the spins are anti-aligned along the chain. The calculated MAE can be found in the Table.I, which indicates the easy-axis lying in the *ab*-plane, i.e. along the *a*-axis [100]. This computational result is consistent with the theoretical prediction for the ground-state spin configuration shown in Ref.[12]. However, as our calculations show in Table.I, the energy gap between the states with spins along [100] and [110] is as small as 0.07 meV/Cr, which is in the order of 1 Kelvin. This quasi-degeneracy could induce interesting physics through quantum fluctuations between these two spin configurations. In addition, the energy between [001] and [100] is also small (~ 0.1 meV), which is ~ 1 Kelvin. This could lead to spin fluctuations between [100] and [001].

We have also performed both the DFT+U and calculations implemented in VASP to study the dependence of exchange interactions between the spins on the Cr ions on the on-site Coulomb U parameter. Here we have adopted a spin Hamiltonian as follows, $\hat{H} = \sum_{\langle i,j \rangle \in \text{Intra, NN}} 2J_{\text{NN}}^{\text{Intra}} \hat{s}_i \cdot \hat{s}_j + \sum_{\langle i,j \rangle \in \text{Intra, NNN}} 2J_{\text{NNN}}^{\text{Intra}} \hat{s}_i \cdot \hat{s}_j + \sum_{\langle i,j \rangle \in \text{Inter, NN}} 2J_{\text{NN}}^{\text{Inter}} \hat{s}_i \cdot \hat{s}_j$. So positive exchange interaction implies anti-ferromagnetic (AFM) coupling, where negative for ferromagnetic (FM) couplings. We can see that the intra-chain exchange interactions will decrease as U increases. The calculated intra-chain NN exchange interaction for $U = 0.5$ (1.0 eV) is (11.6) 8.9 meV, the intra-chain NNN 1.4 (0.9) meV, and the inter-chain coupling -0.02 (-0.01) meV. Both the NN and NNN exchange interaction along the chain is AFM, which suggests an interesting spin frustration in one dimension. Due to the strong quantum fluctuations, this could result in quantum spin liquid in one dimension. Based on the calculations carried out, the optimal U is between 1 and 1.5 eV to fit the experimental effective intra-chain AFM exchange interaction ~ 75 K (6.5 meV), which is the difference between the intra-chain NN and the NNN

exchange interactions within a mean-field approximation. This was derived from the SQUID measurement of $|\theta_p| = 375$ K by using the mean-field expression for θ_p [12]. These results are consistent with the experimentally observed spin configuration, i.e., AFM in the chain but FM between chains [12]. In addition, the inter-chain coupling is much weaker than the intra-chain NN interaction, suggesting a very strong 1D characteristics, which has been evidenced in the magnetic susceptibility, specific heat measurements, and neutron scattering experiments [12]. In addition, the electronic structure and the density of states of BCS are also calculated within DFT+U and shown in Fig.3. The overlap between S p - and Cr d -PDOS suggests a strong hybridization between them. The valence band maximum is dominated by the Ba and S atoms, which would be responsible for the screening. These results are consistent with the calculations and the experimental results for the band gap in Ref.[12]. The size of on-site Coulomb U for $3d$ electrons is normally in the order 10 eV, which is much larger than that in BCS. This implies that the screening effect from the surrounding atoms, especially a large number of Ba atoms, is significant. Another evidence for this important screening effect is that in our VASP calculations we didn't even include the U parameter but still obtained a consistent band gap compared with the experiments [11]. Therefore, this is a spin chain compound close to the edge between

correlated metal and Mott insulator, in which there is rich physics [42].

IV. CONCLUSIONS

In summary, we have computed the electronic structure and magnetic properties of the spin chain compound $\text{Ba}_6\text{Cr}_2\text{S}_{10}$ newly synthesized and characterized experimentally recently. Our predictions for the magnetic properties are in agreement with the experimental observations. The spins are in plane and anti-aligned along the c -axis, as predicted by our VASP calculations taking into account the SOI. The optimal U parameter is ~ 1.0 eV, which is much smaller than the typical value for $3d$ electrons. This suggests there is significant electrostatic screening effect from the surrounding metallic Ba atoms. In addition, the S-ligands play an important role in the dimerisation, which leads to the typical Peierls transition and CDW. We have also computed the spin densities on Cr atoms, which suggests orbital ordering along the chain. In conclusion, $\text{Ba}_6\text{Cr}_2\text{S}_{10}$ is an interesting spin-chain compound close to the boundary between the Mott insulator and correlated metal due to the small U .

-
- [1] A. M. Tsvelik, Quantum Field Theory in Condensed Matter Physics, *Cambridge University Press*, 2010.
- [2] S. Abel, N. Chancellor, and M. Spannowsky, *Phys. Rev. D* **103**, 016008 (2021).
- [3] S. Mishra, G. Catarina, F. Wu, R. Ortiz, D. Jacob, K. Eimre, J. Ma, C. A. Pignedoli, X. Feng, P. Ruffieux, J. Fernández-Rossier and R. Fasel, *Nature* **598**, 287 (2021).
- [4] F. D. M. Haldane, *Phys. Rev. Lett.* **50**, 1153 (1983).
- [5] X. Chen, Z. Gu, and X. Wen, *Phys. Rev. B* **82**, 155138 (2010).
- [6] X. Chen, Z. Gu, and X. Wen, *Phys. Rev. B* **83**, 035107 (2011).
- [7] W. Wu and A. J. Fisher, arXiv: 2011.06899 (2020).
- [8] P. Calabrese and J. Cardy, *J. Stat. Mech.* P06002 (2004).
- [9] G. A. R. van Dalum, A. K. Mitchell, and L. Fritz, *Phys. Rev. B* **102**, 041111(R) (2020).
- [10] C. Ederer and N. A. Spaldin, *Phys. Rev. B* **76**, 214404 (2007).
- [11] J. Zhang, A. C. Komarek, M. Jin, X. C. Wang, Y. T. Jia, J. F. Zhao, W. M. Li, Z. W. Hu, W. Peng, X. Wang, L. H. Tjeng, Z. Deng, R. Z. Yu, S. M. Feng, S. J. Zhang, M. Liu, Y.-F. Yang, H.-j. Lin, C.-T. Chen, X. D. Li, J. L. Zhu, C. Q. Jin, *Phys. Rev. Mater.* **5**, 054606 (2021).
- [12] J. Zhang, X. Wang, L. Zhou, G. Liu, D. T. Adroja, I. Silva, F. Demmel, D. Khalyavin, J. Sannigrahi, H. S. Nair, L. Duan, J. Zhao, Z. Deng, R. Yu, X. Shen, R. Yu, H. Zhao, J. Zhao, Y. Long, Z. Hu, H. Lin, T. Chan, C. Chen, W. Wu, and C. Jin, *Adv. Mater.* **34**, 2106728 (2022).
- [13] C. M. Varma, C. M. (2006), *Phys. Rev. B* **73**, 155113 (2006).
- [14] B. Fauqué, Y. Sidis, V. Hinkov, S. Pailhès, C. T. Lin, X. Chaud, and P. Bourges, *Phys. Rev. Lett.* **96**, 197001 (2006).
- [15] L. Ungur, S. K. Langley, T. N. Hooper, B. Moubaraki, E. K. Brechin, K. S. Murray, L. F. Chibotaru, *J. Am. Chem. Soc.* **134**, 18554 (2012).
- [16] J. F. Wu, X. L. Li, M. Guo, L. Zhao, Y. Q. Zhang, J. K. Tang, *Chem. Commun.*, **54**, 1065 (2018).
- [17] S. Bose, *Contemporary Physics*, **48**, 13 (2007).
- [18] S. Heutz, C. Mitra, Wei Wu, A. J. Fisher, A. Kerridge, A. M. Stoneham, A. H. Harker, J. Gardener, H.-H. Tseng, T. S. Jones, C. Renner, and G. Aeppli, *Adv. Mater.* **19**, 3618 (2007).
- [19] W. Wu, A. Kerridge, A. H. Harker and A. J. Fisher, *Phys. Rev. B* **77**, 184403 (2008).
- [20] H. Wang, S. Mauthoor, S. Din, J. A. Gardener, R. Chang, M. Warner, G. Aeppli, D. W. McComb, M. P. Ryan, Wei Wu, A. J. Fisher, A. M. Stoneham and S. Heutz, *ACS Nano* **4**, 3921 (2010).
- [21] W. Wu, A. J. Fisher, and N. M. Harrison, *Phys. Rev. B* **84**, 024427 (2011).
- [22] M. Serri, W. Wu, L. Fleet, N. M. Harrison, C. W. Kay, A. J. Fisher, C. Hirjibehedin, G. Aeppli, S. Heutz, *Nat. Commun.* **5**, 3079 (2014).
- [23] W. Wu, N. M. Harrison, and A. J. Fisher, *Phys. Rev. B* **88**, 024426 (2013).
- [24] W. Wu, N. M. Harrison, and A. J. Fisher, *Phys. Rev. B (Rap. Comm.)* **88**, 180404(R) (2013).
- [25] W. Wu, A. J. Fisher, and N. M. Harrison, *Phys. Rev. B*

- 88**, 224417 (2013).
- [26] W. Wu, *J. Phys. Cond. Matt.* **26**, 296002 (2014).
- [27] L. Bogani, A. Vindigni, R. Sessolia and D. Gatteschi, *J. Mater. Chem.*, **18**, 4750 (2008).
- [28] W. B. Yelon, D. E. Cox, and M. Eibschütz, *Phys. Rev. B* **12**, 5007 (1975).
- [29] S. Agrestini, L. C. Chapon, A. Daoud-Aladine, J. Schefer, A. Gukasov, C. Mazzoli, M. R. Lees, and O. A. Petrenko, *Phys. Rev. Lett.* **101**, 097207 (2008).
- [30] S. Toth, W. Wu, D. T. Adroja, S. Rayaprol, E. V. Sampathkumaran, *Phys. Rev. B* **93**, 174422 (2016).
- [31] M. Mao, B. D. Gaulin, R. B. Rogge, and Z. Tun, *Phys. Rev. B* **66**, 184432 (2002).
- [32] A. D. Hillier, D. T. Adroja, W. Kockelmann, L. C. Chapon, S. Rayaprol, P. Manuel, H. Michor, and E. V. Sampathkumaran, *Phys. Rev. B* **83**, 024414 (2011).
- [33] W.-G. Yin, X. Liu, A. M. Tselik, M. P. M. Dean, M. H. Upton, J. Kim, D. Casa, A. Said, T. Gog, T. F. Qi, G. Cao, and J. P. Hill, *Phys. Rev. Lett.* **111**, 057202 (2013).
- [34] E. V. Sampathkumaran, N. Mohapatra, S. Rayaprol, and K. K. Iyer, *Phys. Rev. B* **75**, 052412 (2007).
- [35] T. Basu, K. Iyer, K. Singh, K. Mukherjee, P. Paulose, and E. Sampathkumaran, *Appl. Phys. Lett.* **105**, 102912 (2014).
- [36] P. E. Blöchl, *Phys. Rev. B* **50**, 17953 (1994).
- [37] G. Kresse and J. Furthmüller, *Comput. Mater. Sci* **6**, 15 (1996).
- [38] G. Kresse and J. Furthmüller, *Phys. Rev. B* **54**, 11169 (1996).
- [39] J. P. Perdew, K. Burke, and M. Ernzerhof, *Phys. Rev. Lett.* **77**, 3865 (1996).
- [40] D. Vanderbilt, *Phys. Rev. B* **41** (Rapid Communications), 7892 (1990).
- [41] H. J. Monkhorst and J. D. Pack, *Phys. Rev. B* **13**, 5188 (1976).
- [42] G. Kotliar, S. Y. Savrasov, K. Haule, V. S. Oudovenko, O. Parcollet, and C. A. Marianetti, *Rev. Mod. Phys.* **78**, 865 (2006).

ACKNOWLEDGEMENTS

WW wishes to acknowledge the funding support from EU Horizon 2020 Marketplace project No.760173. We thank the inspiring discussion with Prof. Changqing Jin and Prof. Xiancheng Wang.